Electronic Supplementary Material (ESI) for Inorganic Chemistry Frontiers.

Modulating Anthracene Excimer through Guest Engineering in Two-Dimensional Lead Bromide Hybrids

Xiaohui Liu[a,†], Xianli Li[b,†], Jie Li[a], Xin Lian[a], Yonghong Xiao[a], Ruosheng Zeng[c], Shao-Fei Ni[a], Ke Xu[d], Yan Kuai[e,*], Wen-Xiu Ni[b] and Binbin Luo[a,*]

[a] *Department of Chemistry and Key Laboratory for Preparation and Application of Ordered Structural Materials of Guangdong Province, Shantou University, Shantou 515063, P. R. China*

[b] *Department of Medicinal Chemistry, Shantou University Medical College, Shantou 515041, P. R. China*

[c] *School of Physical Science and Technology, State Key Laboratory of Featured Metal Materials and Life-cycle Safety for Composite Structures, Guangxi University, Nanning 530004, P. R. China*

[d] *Multiscale Crystal Materials Research Center, Shenzhen Institute of Advanced Technology, Chinese Academy of Sciences, Shenzhen 518055, P. R. China*

[e] *Information Materials and Intelligent Sensing Laboratory of Anhui Province, Anhui University, Hefei 230601, P. R. China*

Email: yankuai@ahu.edu.cn; bbluo@stu.edu.cn

EXPERIMENTAL SECTION

Materials and methods

10-chloro-9-anthraldehyde (97%, Bide Pharmatech Ltd.), formic acid (96%, Aladdin), hydrogen bromide (48%, Energy Chemical), ethyl acetate (AR, Xilong Scientific), N,N-dimethylformamide (DMF, AR, Xilong Scientific), dimethyl sulfoxide (DMSO, AR, Xilong Scientific), ammonium hydroxide (AR, Xilong Scientific), sodium hydroxide (48%, Energy Chemical), hydrochloric acid (36%, Xilong Scientific), methanol (AR, Xilong Scientific), ethanol (AR, Xilong Scientific), 1-Propanol (AR, Xilong Scientific), 1-butanol (99%, Aladdin), 1-pentanol (98%, Aladdin), 1-hexanol (99%, Aladdin), 1-heptanol (99%, Aladdin), 1-decanol (99%, Aladdin), 1-nonanol (98%, Aladdin), 1-decylalcohol (98%, Aladdin), all chemicals were used without further purification.

Synthesis of 9-dimethylaminomethyl-10-chloroanthracene (DCAn)

First, 10-chloro-9-anthraldehyde (5.8 g), HCOOH (10 g), and DMF (20 mL) were added into 100 mL round-bottled flask and then refluxed at 150-160 ℃ for 5 hours. After the solution is cooled down to room temperature, 20 wt.% NaOH (80 mL) was added into the above solution to precipitate the solute. The resulting solids were obtained by filtering and then dried at 60 °C. At last, the dried solids were dissolved in ethyl acetate and extracted with 0.1 mol/L HCl solution for 4 times. Finally, aqueous ammonia was added into the HCl solution until the formation of yellow solids.

Synthesis of (DCAn)Br powders

DCAn (26.9 mg) was dissolved into 2 mL ethyl acetate. Then, the DCAn ethyl acetate solution will turn into muddy after adding 2 drops of HBr solution. (DCAn)Br can be obtained after filtering and the powders were rinsed with ethyl acetate for three times.

Synthesis of DCAn and (DCAn)Br single crystal

DCAn powders (0.0269 g) were first dissolved into 5 mL methanol in an open vial and DCAn single crystal will be obtained after keeping the solution standing for at least 24 h. As for (DCAn)Br single crystal, DCAn powders (0.0269 g) were dissolved into 3 mL DMSO, then 50 μL HBr solution is directly added into the DMSO solution. (DCAn)Br single crystal will be obtained after keeping the mixed solution standing for at least 6 h.

Synthesis of 1-CX single crystal

First, 0.10 mmol $PbBr_2$ was dissolved in 2 mL HBr and 0.13 mmol DCAn was dissolved in 20 mL

methanol. Then the HBr solution is directly added into the DCAn methanol solution. The 1-C1 single crystal will be obtained after keeping the mixed solution standing for at least 8 h. Similarly, 1-CX ($2 \leq X \leq 8$) single crystals can be harvested through the same method except that the volume of the corresponding alcohol solution and the standing time was increased into 60 mL and 48 h, respectively.

Activation of 1-CX single crystal

1-CX-act. are obtained by placing 1-C1 crystals in a 10 mL Schlenk tube with vacuum treatment for 5 hours at 110 ℃.

Characterization

Single crystal X-ray diffraction (SC-XRD). SC-XRD tests were conducted on Rigaku XtaLab Pro MM007HF DWX diffractometer at 298 K and 100K using Cu Kα radiation (λ = 1.5418 Å). The structures were solved by intrinsic phasing method using SHELXT[1] program implanted in Olex2[2]. Refinement with full matrix least squares techniques on F^2 was performed by using SHELXL[3]. Non-hydrogen atoms were anisotropically refined and all hydrogen atoms were generated based on riding mode.

Powder XRD. PXRD patterns were recorded on MiniFlex 600 (Rigaku) to examine the crystalline phase.

UV-vis absorption. UV-vis spectra were measured on Lambda 950 UV-vis Spectrometer (PerkinElmer).

Photoluminescence (PL) and excitation (PLE) spectra. Both of PL and PLE spectra were collected on PTI QM-TM (Photon Technology International).

Absolute PL quantum yield (QY). Absolute PL QY was recorded on a HAMAMATSU C11347 spectrometer with integrating sphere with the excitation wavelength of 380 nm for all samples.

Photoluminescence lifetime. PL lifetime tests were collected on Edinburgh Instruments (FL 980). The PL decay curves are fitted with exponential function as given in the following expression:

$$I(t) = \sum_{n}^{i=1} A_i e^{-\frac{t}{\tau_i}}$$

where $I(t)$ is the PL intensity at time t, A_i represents the relative weights of the decay components, τ_i denotes the decay time for the exponential components. The average lifetime is calculated based on the expression below:

$$\tau_{ave} = \sum_{n}^{i=1} A_i \tau_i^2 \Big/ \sum_{n}^{i=1} A_i \tau_i$$

Optical waveguide. The single longitudinal mode 405 nm laser (MDL-C-405, CNI Co., Ltd) was used to excite the fluorescence of optical waveguide. First, the laser beam after expansion and collimation was focused on the surface of the substrate through a condenser (ACL2520U-A, Thorlabs, Inc). Driven by a three-axis linear stage (PT3A/M, Thorlabs, Inc), the condenser accurately focused the light spot at different positions with equal spacing on the micron optical waveguide, so as to measure the transmission characteristics of the nanometer optical waveguide. A home-made inverted microscope used an apochromatic objective (PLN10X, Olympus, Inc) to collect fluorescence signals and imaged them with a highly sensitive sCMOS camera (Dhyana 400D, Tucsen, Inc). An additional long-pass filter (FELH0450, Thorlabs, Inc) is added in front of the tube mirror to eliminate the influence of excitation light on the measurement results.

Computational methodology. To study the effect of alcohol guests on the configuration of An dimers and the optical properties of $(DCAn)_4Pb_3Br_{10}\cdot 2CH_3(CH_2)_{X\text{-}1}OH$, first-principles calculations were carried out using density functional theory (DFT) as implemented in the VASP code.[4-5] The projector augmented wave (PAW) method was used to describe the interaction between ions and electrons.[6] The structural optimization were calculated using Perdew-Burke-Ernzerhof (PBE) exchange-correlation functional.[7] The simulated model are modified by using primitive cell. The Brillouin zone integration was sampled with 2×3×2 K-point meshes for static calculations. Following the space group of these structures, the K points of Brillouin region were referred to the symmetry of their space group to calculate band structure and density of states. The energy cutoff of plane-wave basis is 500 eV. The residual force of all atoms in the models was less than 0.02 eV/Å.

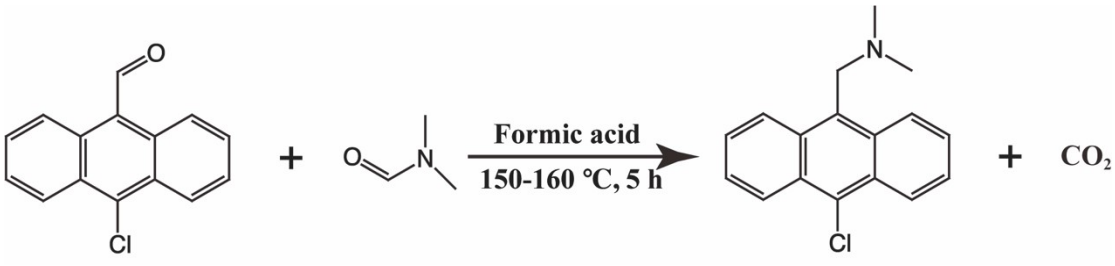

Figure S1. The synthetic route of DCAn.

Table S1. Crystal data of DCAn and (DCAn)Br.

Sample	DCAn	(DCAn)Br
Empirical formula	$C_{17}H_{16}ClN$	$C_{17}H_{17}ClNBr$
Formula weight	269.76	350.67
Temperature/K	262.0	300.10(10)
Radiation	Cu Kα (λ = 1.54178)	Cu Kα (λ = 1.54184 Å)
Crystal system	monoclinic	monoclinic
Space group	$P2_1/n$	$P2_1/n$
a/Å	9.3418(6)	10.55490(10)
b/Å	10.7903(6)	13.17590(10)
c/Å	14.0401(8)	11.98320(10)
α/°	90	90
β/°	100.427(2)	113.4820(10)
γ/°	90	90
V/Å^3	1391.88(14)	1528.50(2)
Z	4	4
ρ_{calc} (g/cm^3)	1.287	1.524
completeness to θ_{max}	99.3%	96.4%
GOF	1.160	1.052
R_{int}	0.0808	0.0193
final R indexes [$I > 2\sigma(I)$][a]	$R_1 = 0.1032$, $wR_2 = 0.2547$	$R_1 = 0.0250$, $wR_2 = 0.0661$
R indexes (all data)[a]	$R_1 = 0.1417$, $wR_2 = 0.2797$	$R_1 = 0.0269$, $wR_2 = 0.0674$
largest diff. peak and hole, e Å^{-3}	1.04/-0.61	0.26/-0.32

[a] $R_1 = \Sigma||F_o|-|F_c||/\Sigma|F_o|$; $wR_2 = \{[\Sigma w(F_o^2-F_c^2)^2]/\Sigma[w(F_o^2)^2]\}^{1/2}$; $w = 1/[\sigma^2 (F_o^2)+(aP)^2 +bP]$, where $P = [\max(F_o^2, 0) + 2Fc^2]/3$ for all data.

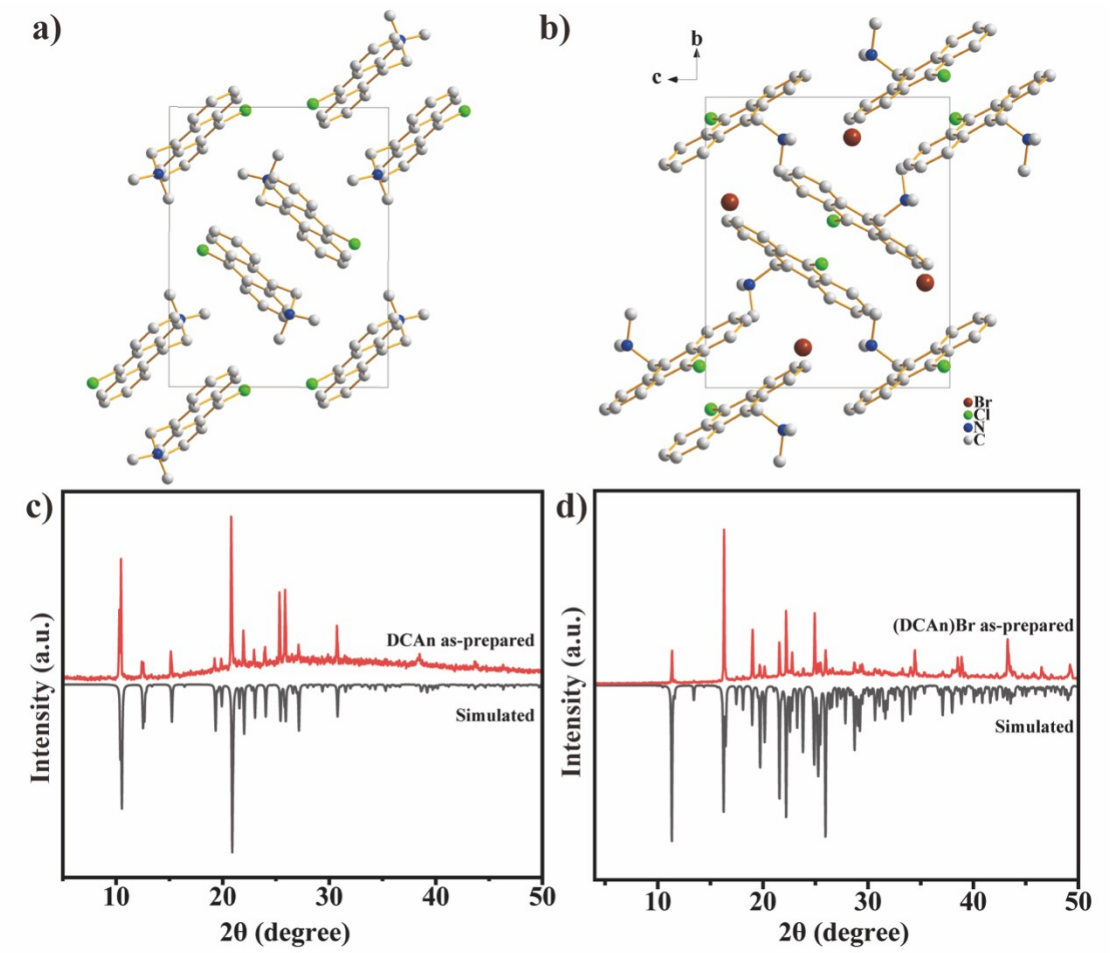

Figure S2. Crystal structures and XRD patterns of DCAn (a, c) and (DCAn)Br (b, d).

Table S2. Crystal data of 1-C1, 1-C2 and 1-C3.

Sample	1-C1	1-C2	1-C3
Empirical formula	$(C_{17}H_{17}ClN)_4Pb_3Br_{10}\cdot 2CH_3OH$	$(C_{17}H_{17}ClN)_4Pb_3Br_{10}\cdot 2C_2H_5OH$	$(C_{17}H_{17}ClN)_4Pb_3Br_{10}\cdot 2C_3H_7OH$
Formula weight	2567.81	2595.87	2623.92
Temperature/K	297.98(10)	297.99(10)	297.98(10)
Radiation	Cu *K*α (λ = 1.54184 Å)	Cu *K*α (λ = 1.54184 Å)	Cu Kα (λ = 1.54184 Å)
Crystal system	monoclinic	monoclinic	monoclinic
Space group	*C*2/*c*	*C*2/*c*	*C*2/*c*
a/Å	21.3980(3)	21.4608(3)	21.4204(5)
b/Å	9.82910(10)	9.8836(2)	9.8038(2)
c/Å	38.8397(5)	39.2773(6)	40.7386(9)
α/°	90	90	90
β/°	100.8460(10)	98.840(2)	92.275(2)
γ/°	90	90	90
V/Å^3	8022.96(18)	8232.1(2)	8548.4(3)
Z	4	4	4
ρ_{calc} (g/cm^3)	2.126	2.094	2.039
completeness to θ_{max}	96.2%	96.2%	96.1%
GOF	1.046	1.032	1.037
R_{int}	0.0259	0.0268	0.0366
final *R* indexes [$I > 2\sigma(I)$][a]	$R_1 = 0.0236$, $wR_2 = 0.0596$	$R_1 = 0.0291$, $wR_2 = 0.0756$	$R_1 = 0.0479$, $wR_2 = 0.1400$
R indexes (all data)[a]	$R_1 = 0.0270$, $wR_2 = 0.0609$	$R_1 = 0.0319$, $wR_2 = 0.0771$	$R_1 = 0.0546$, $wR_2 = 0.1450$
largest diff. peak and hole, e Å^{-3}	0.60/-0.80	1.15/-0.76	1.98/-1.80

[a] $R_1 = \Sigma||F_o|-|F_c||/\Sigma|F_o|$; $wR_2 = \{[\Sigma w(F_o^2-F_c^2)^2]/\Sigma[w(F_o^2)^2]\}^{1/2}$; $w = 1/[\sigma^2(F_o^2)+(aP)^2+bP]$, where $P = [\max(F_o^2, 0) + 2Fc^2]/3$ for all data.

Table S3. Crystal data of 1-C4, 1-C5 and 1-C6.

Sample	1-C4	1-C5	1-C6
Empirical formula	$(C_{17}H_{17}ClN)_4Pb_3Br_{10}\cdot 2C_4H_9OH$	$(C_{17}H_{17}ClN)_4Pb_3Br_{10}\cdot 2C_5H_{11}OH$	$(C_{17}H_{17}ClN)_4Pb_3Br_{10}\cdot 2C_6H_{13}OH\cdot 2H_2O$
Formula weight	2651.97	2680.02	2744.10
Temperature/K	296.42(12)	297.99(10)	100.00(10)
Radiation	Cu Kα (λ = 1.54184 Å)	Cu Kα (λ = 1.54184 Å)	Cu Kα (λ = 1.54184 Å)
Crystal system	monoclinic	monoclinic	monoclinic
Space group	*C*2/*c*	*C*2/*c*	$P2_1/c$
a/Å	21.4718(2)	21.5945(4)	22.6272(3)
b/Å	9.80050(10)	9.8290(2)	9.91720(10)
c/Å	40.8581(5)	41.2029(10)	22.1336(3)
α/°	90	90	90
β/°	92.2310(10)	92.467(2)	117.360(2)
γ/°	90	90	90
V/Å^3	8591.43(16)	8737.3(3)	4411.15(12)
Z	4	4	2
ρ_{calc} (g/cm^3)	2.050	2.037	2.066
completeness to θ_{max}	96.7%	96.6%	96.9%
GOF	1.068	1.071	1.025
R_{int}	0.0233	0.0240	0.0395
final *R* indexes $[I > 2\sigma(I)]$[a]	$R_1 = 0.0247$, $wR_2 = 0.0591$	$R_1 = 0.0301$, $wR_2 = 0.0809$	$R_1 = 0.0344$, $wR_2 = 0.0933$
R indexes (all data)[a]	$R_1 = 0.0267$, $wR_2 = 0.0601$	$R_1 = 0.0330$, $wR_2 = 0.0825$	$R_1 = 0.0373$, $wR_2 = 0.0957$
largest diff. peak and hole, e Å^{-3}	0.70/-1.25	0.74/-1.01	2.28/-2.38

[a] $R_1 = \Sigma||F_o|-|F_c||/\Sigma|F_o|$; $wR_2 = \{[\Sigma w(F_o^2-F_c^2)^2]/\Sigma[w(F_o^2)^2]\}^{1/2}$; $w = 1/[\sigma^2(F_o^2)+(aP)^2+bP]$, where $P = [\max(F_o^2, 0) + 2Fc^2]/3$ for all data.

Table S4. Crystal data of 1-C7, 1-C8 and 1-C9.

Sample	1-C7	1-C8	1-C9
Empirical formula	$(C_{17}H_{17}ClN)_4Pb_3Br_{10}\cdot 2C_7H_{15}OH\cdot 2H_2O$	$(C_{17}H_{17}ClN)_4Pb_3Br_{10}\cdot 2C_8H_{17}OH\cdot 2H_2O$	$(C_{17}H_{17}ClN)_6Pb_5Br_{16}\cdot 4C_9H_{19}OH\cdot 2H_2O$
Formula weight	2772.16	2800.21	4552.13
Temperature/K	100.00(10)	100.00(10)	100.00(10)
Radiation	Cu Kα (λ = 1.54184 Å)	Cu Kα (λ = 1.54184 Å)	Cu Kα (λ = 1.54184 Å)
Crystal system	monoclinic	monoclinic	triclinic
Space group	$P2_1/c$	$P2_1/c$	P-1
a/Å	22.5955(4)	22.4859(2)	9.5838(2)
b/Å	9.98480(10)	10.01480(10)	19.9092(4)
c/Å	22.1409(4)	22.3690(2)	20.8586(2)
α/°	90	90	100.8410(10)
β/°	115.695(2)	114.2300(10)	101.844(2)
γ/°	90	90	91.795(2)
V/Å^3	4501.29(14)	4593.55(8)	3815.55(12)
Z	2	2	1
ρ_{calc} (g/cm^3)	2.045	2.025	1.981
completeness to θ_{max}	95.8%	97.2%	96.1%
GOF	1.073	1.058	1.052
R_{int}	0.0282	0.0304	0.0347
final R indexes $[I > 2\sigma(I)]$[a]	$R_1 = 0.0324$, $wR_2 = 0.0965$	$R_1 = 0.0359$, $wR_2 = 0.0942$	$R_1 = 0.0331$, $wR_2 = 0.0904$
R indexes (all data)[a]	$R_1 = 0.0346$, $wR_2 = 0.0981$	$R_1 = 0.0382$, $wR_2 = 0.0957$	$R_1 = 0.0360$, $wR_2 = 0.0922$
largest diff. peak and hole, e Å^{-3}	1.72/-2.91	3.94/-1.48	2.73/-1.68

[a] $R_1 = \Sigma||F_o|-|F_c||/\Sigma|F_o|$; $wR_2 = \{[\Sigma w(F_o^2-F_c^2)^2]/\Sigma[w(F_o^2)^2]\}^{1/2}$; $w = 1/[\sigma^2(F_o^2)+(aP)^2+bP]$, where $P = [\max(F_o^2, 0) + 2Fc^2]/3$ for all data.

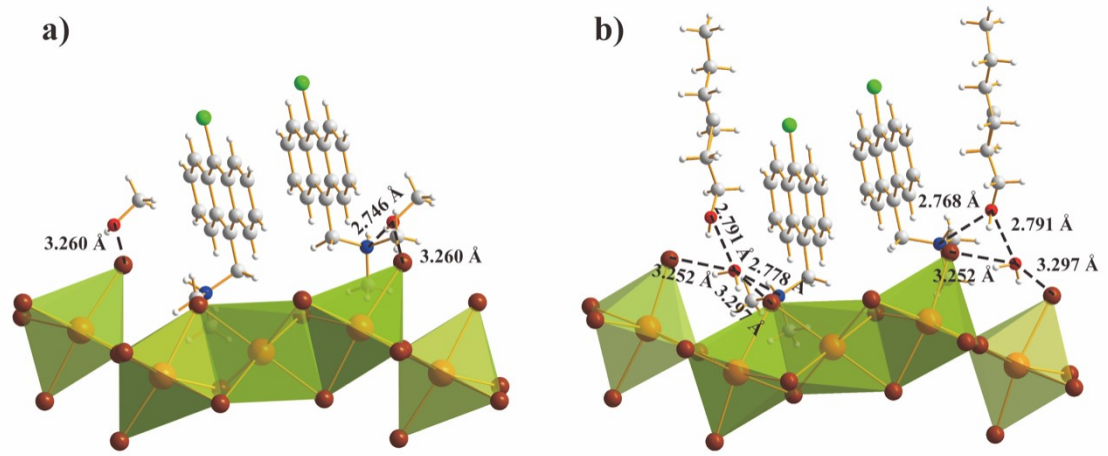

Figure S3. The hydrogen bonding interaction between DCAn and inorganic layers in (a) 1-C1 and (b) 1-C6.

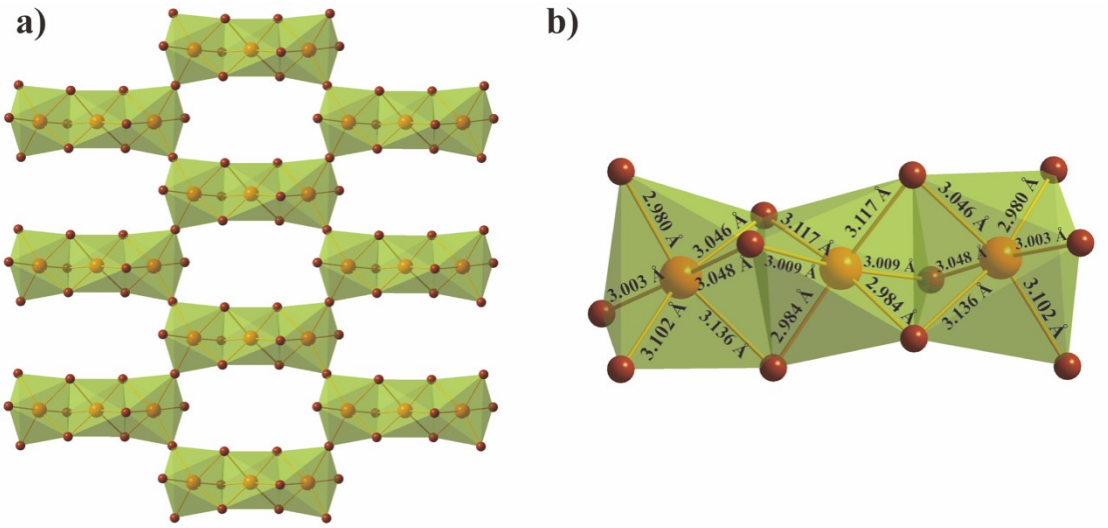

Figure S4. Crystal structure of (a) inorganic layers and (b) face-shared [Pb_3Br_{12}] trimers of 1-C1.

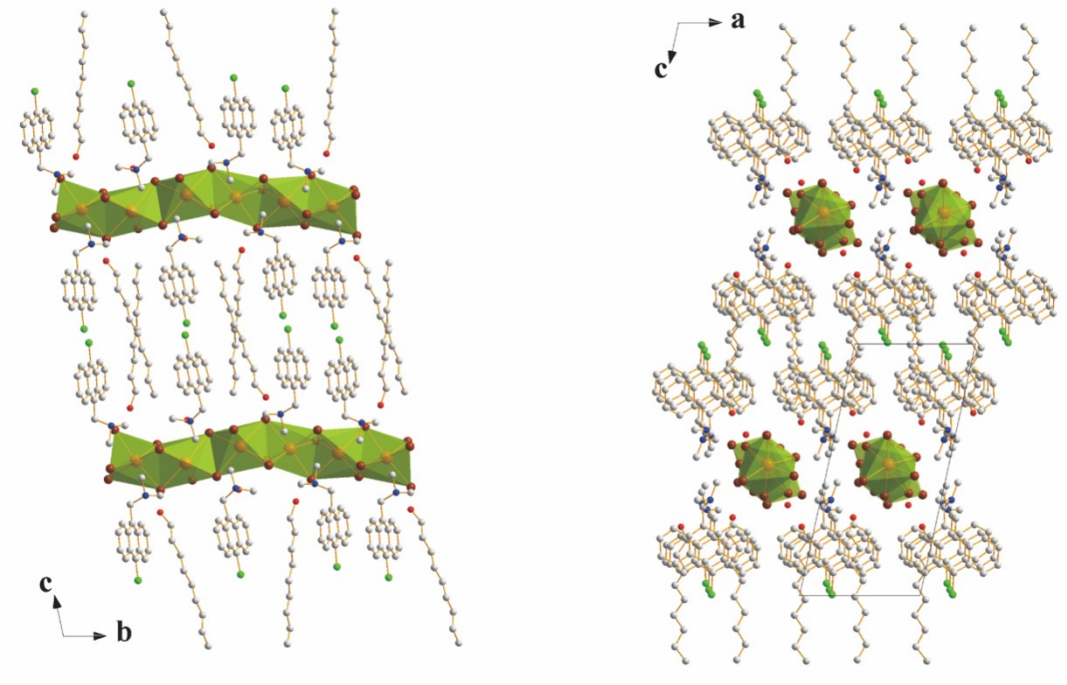

Figure S5. Crystal structure of 1-C9 from different viewing direction. Pb (orange), Br (dark red), Cl (green), N (blue), O (red) and C (gray).

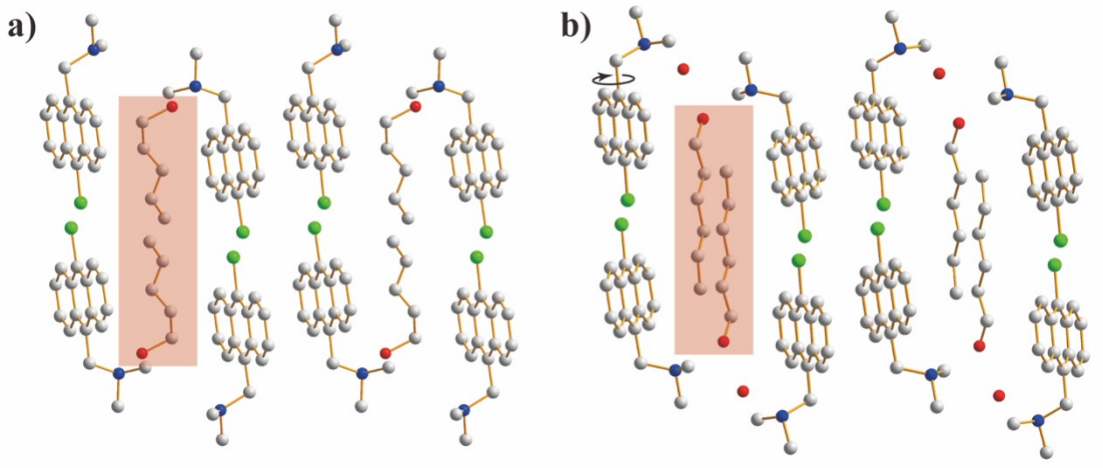

Figure S6. The difference (highlighted with red color) of alcohol guests inserted in adjacent organic layers for (a) 1-C5 and (b) 1-C6. Cl (green), N (blue), O (red) and C (gray).

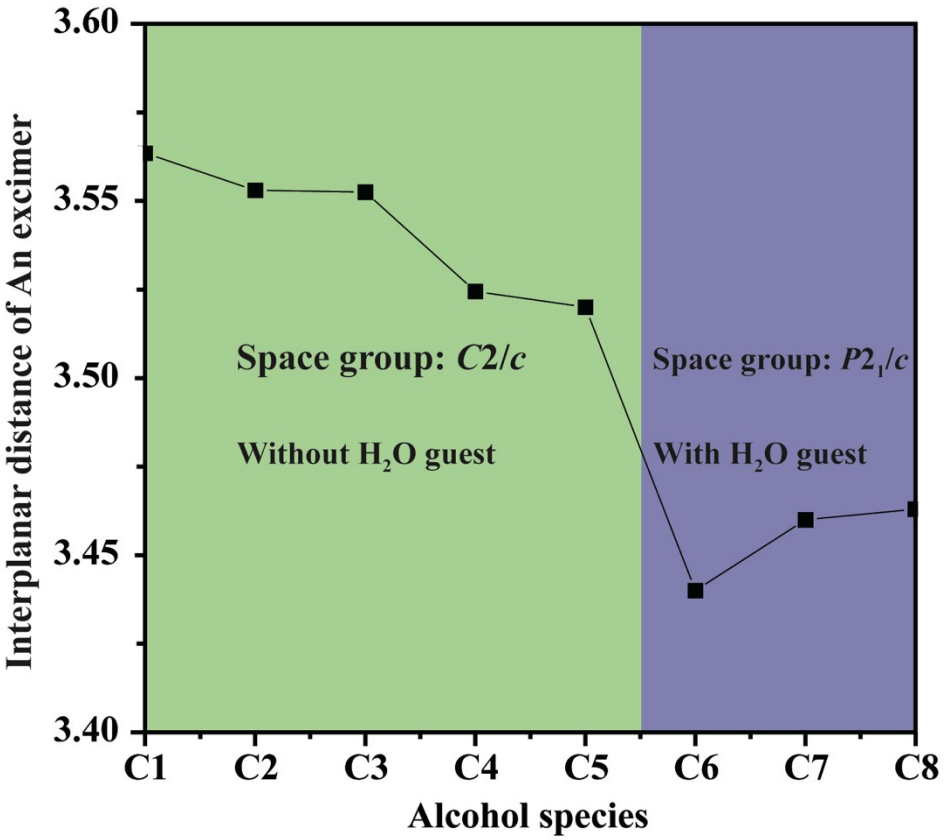

Figure S7. Correlation of the average interplanar distance of An dimers with alcohol species.

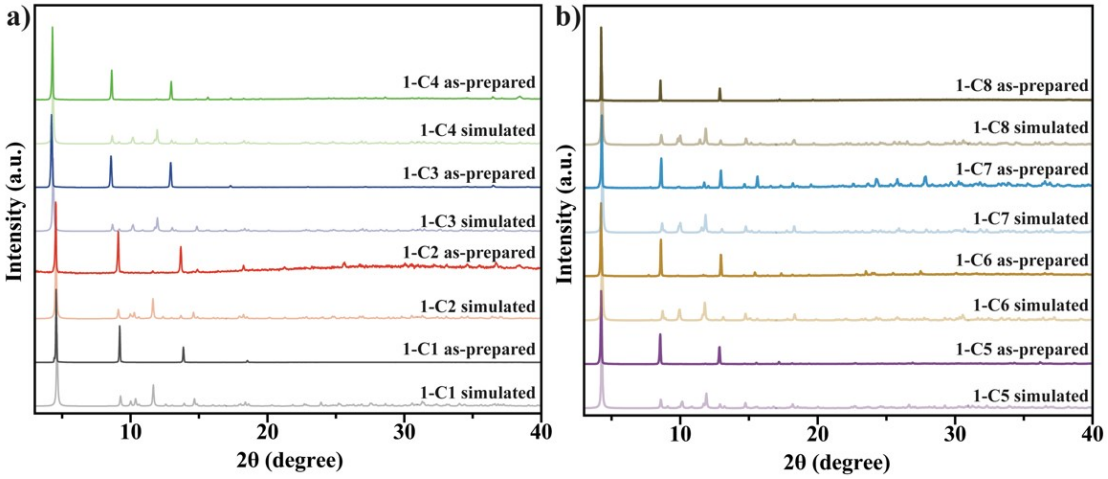

Figure S8. XRD patterns of 1-CX.

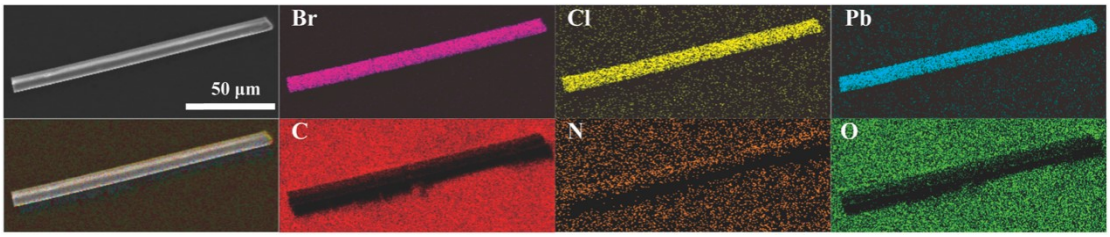

Figure S9. SEM images and EDS mapping of 1-C6.

Since the sample is deposited on conductive adhesive, a higher concentration of C, N, O is observed in the area without sample.

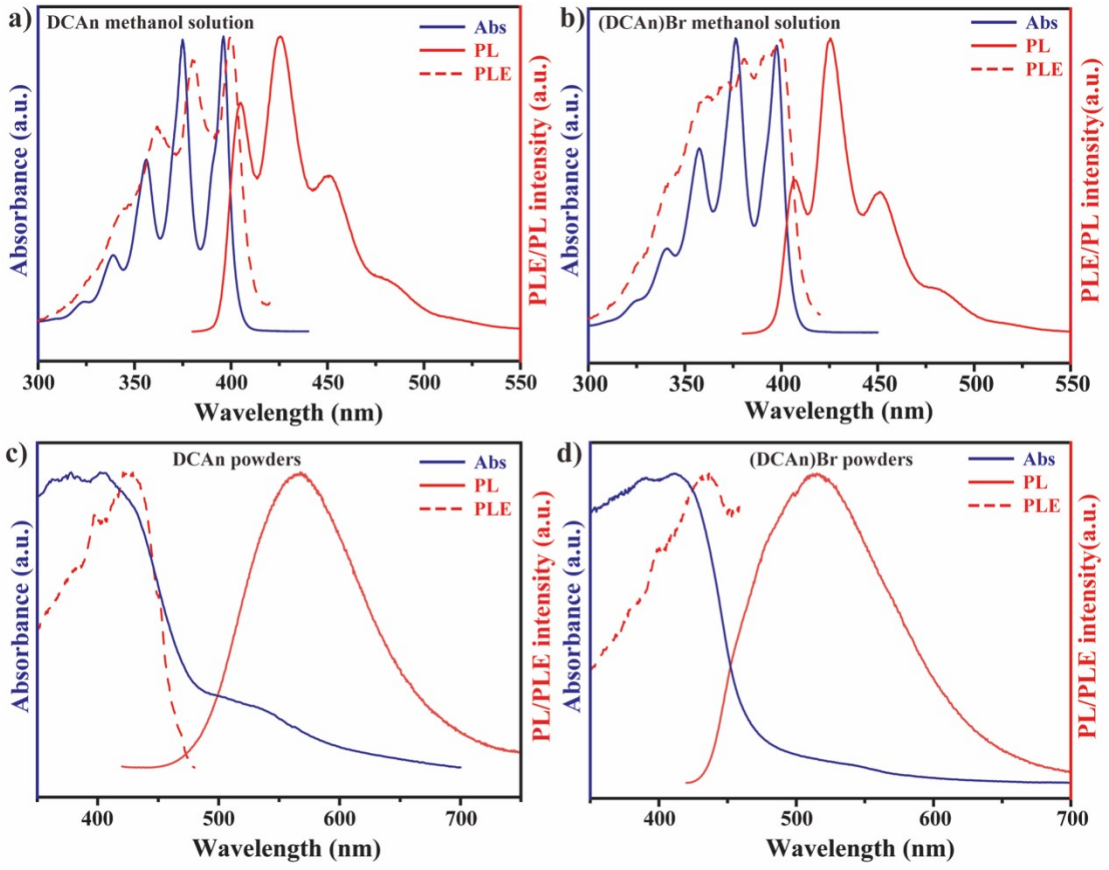

Figure S10. Absorption, PL and PLE spectra of (a) DCAn methanol solution, (b) (DCAn)Br methanol solution, (c) DCAn powders and (DCAn)Br powders.

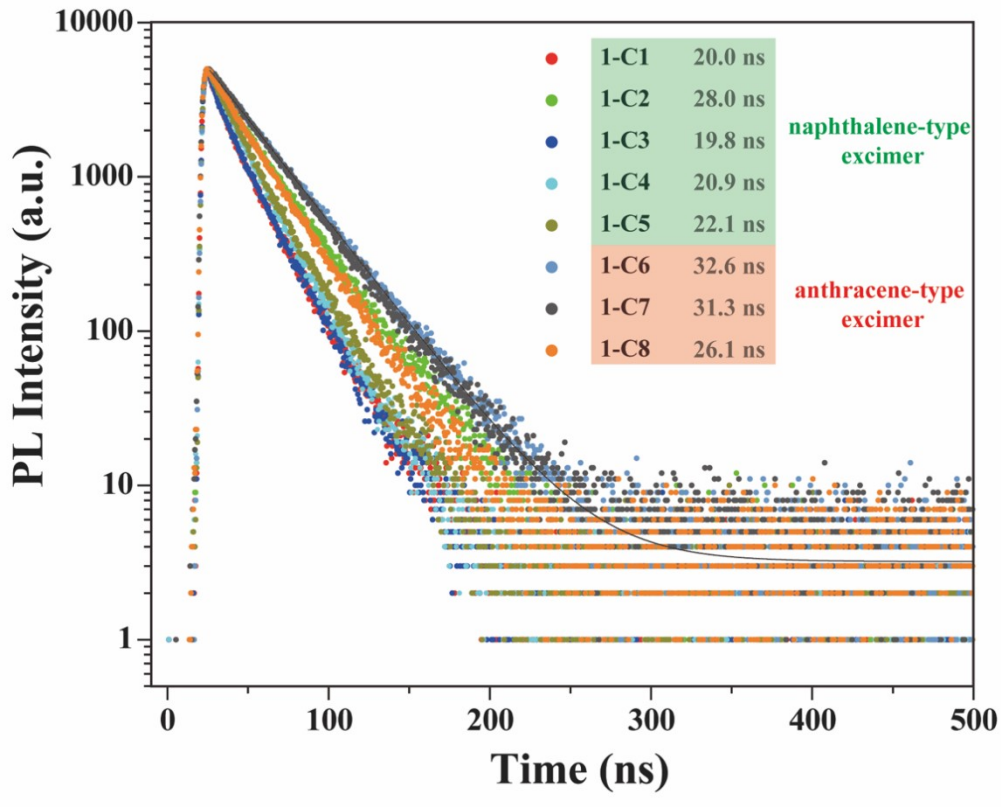

Figure S11. PL lifetime tests of 1-CX with 400 nm excitation.

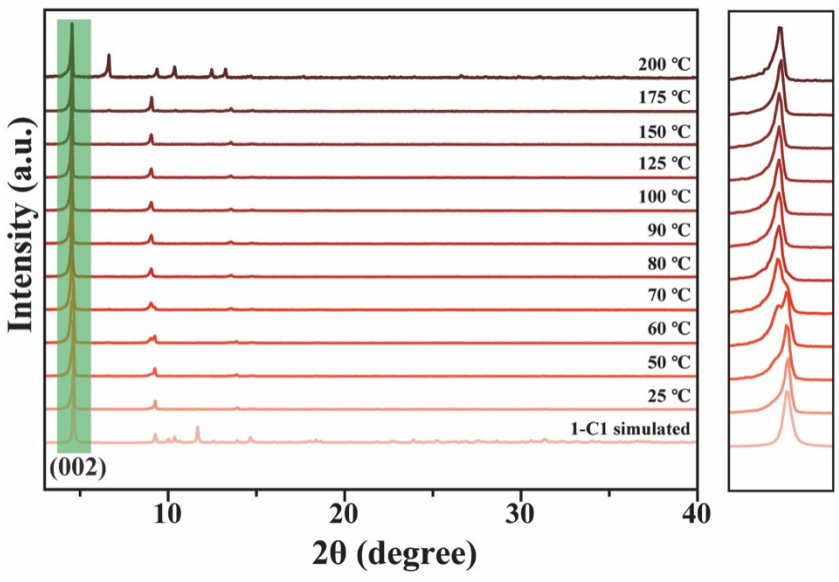

Figure S12. T-dependent XRD of 1-C1.

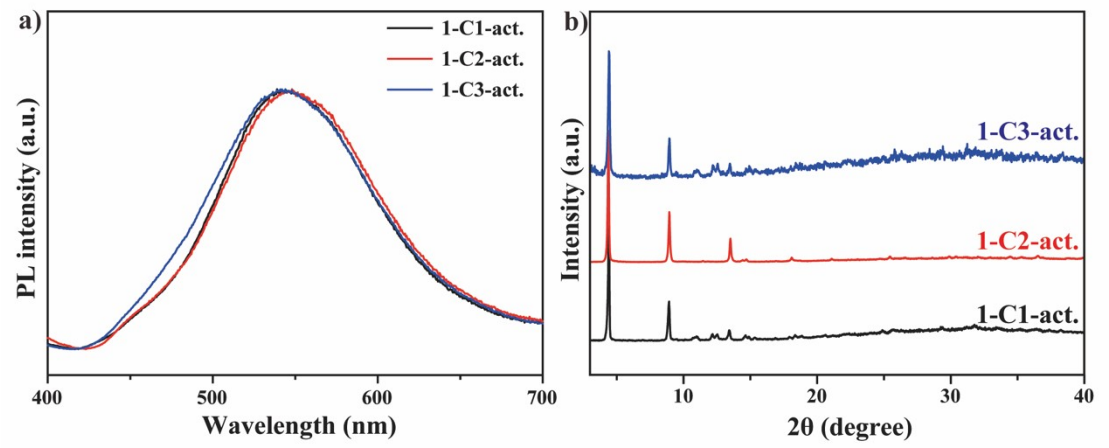

Figure S13. (a) PL spectra and (b) XRD of 1-C1-act., 1-C2-act. and 1-C3-act..

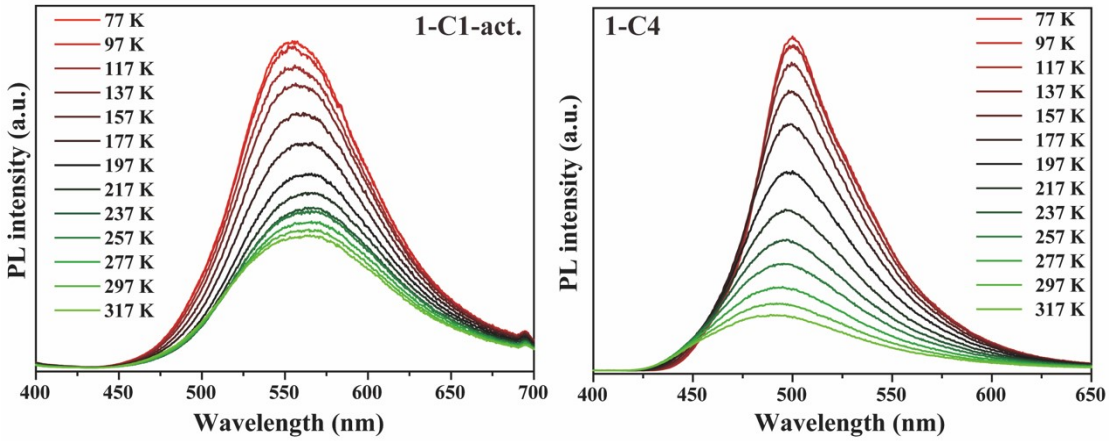

Figure S14. T-dependent PL spectra of 1-C1-act. and 1-C4.

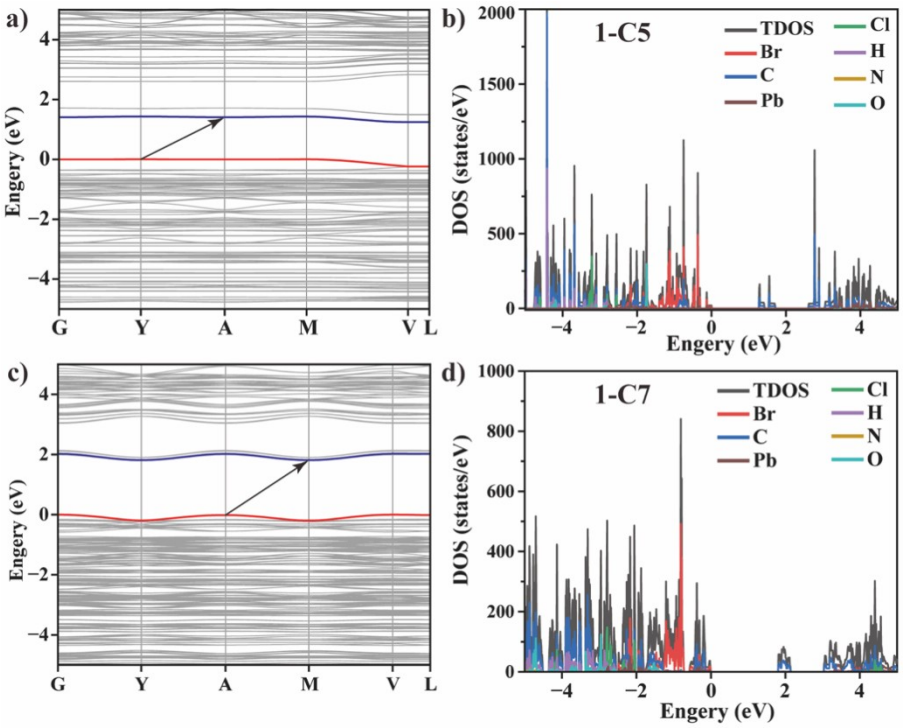

Figure S15. Calculated band structure and TDOS of (a, b) 1-C5 and (c, d) 1-C7.

Table S5. Comparison of the performance of optical waveguide between reported works and our work.

Sample name	Wavelength/nm	OLC/dB mm^{-1}	Ref.
1-C5	493	3.11	this work
1-C7	552	2.68	
$(PTMA)_3Cu_3I_6$	614	15.7	8
$(H_2TTz)ZnCl_4·MeOH$	462	15.77	9
$(H_2TTz)·ZnBr_4·MeOH$	515	11.82	
$(DTA)_2SbCl_5·DTAC$	620	1.92	10
$ZnCl_2$-B	~420-570	1.0	11
Zn-Bpeb	595	0.893	12
Cd-Bpeb	583	0.308	
Pb-Bpeb	692	9.08	
$(KC)MnCl_4$	518	9.93	13
OIHP-AD	533	4	14
Eu-BTC	615	12	15

REFERENCES

1. Sheldrick, G. M., Shelxt - Integrated Space-Group and Crystal-Structure Determination. *Acta Cryst. A* **2015**, *71*, 3-8.

2. Dolomanov, O. V. B., L. J.; Gildea, R. J.; Howard, J. A. K.; Puschmann, H., Olex2: A Complete Structure Solution, Refinement and Analysis Program. *J. Appl. Crystallogr.* **2009**, *42*, 339-341.

3. Sheldrick, G. M., A Short History of Shelx. *Acta Cryst. A* **2008**, *64*, 112-122.

4. Furthmüller, G. K. a. J., Efficient Iterative Schemes for Ab Initio Total-Energy Calculations Using a Plane-Wave Basis Set. *Phys. Rev. B* **1996**, *54*, 11169-11186.

5. Joubert, G. K. a. D., From Ultrasoft Pseudopotentials to the Projector Augmented-Wave Method. *Phys. Rev. B* **1999**, *59*, 1758-1775.

6. Blöchl, P. E., Projector Augmented-Wave Method. *Phys. Rev. B* **1994**, *50*, 17953-17979.

7. John P. Perdew, K. B., and Matthias Ernzerhof, Generalized Gradient Approximation Made Simple. *Phys. Rev. Lett.* **1996**, *77*, 3865-3868.

8. Lian, L.; Zhang, T.; Ding, H.; Zhang, P.; Zhang, X.; Zhao, Y.-B.; Gao, J.; Zhang, D.; Zhao, Y. S.; Zhang, J., Highly Luminescent Zero-Dimensional Organic Copper Halide with Low-Loss Optical Waveguides and Highly Polarized Emission. *ACS Materials Lett.* **2022**, *4*, 1446-1452.

9. Li, K.-J.; Zhao, Y.-Y.; Sun, M.-E.; Chen, G.-S.; Zhang, C.; Liu, H.-L.; Li, H.-Y.; Zang, S.-Q.; Mak, T. C. W., Zero-Dimensional Zinc Halide Organic Hybrids with Excellent Optical Waveguide Properties. *Cryst. Growth Des.* **2022**, *22*, 3295-3302.

10. Liu, F., et al., Light-Emitting Metal-Organic Halide 1d and 2d Structures: Near-Unity Quantum Efficiency, Low-Loss Optical Waveguide and Highly Polarized Emission. *Angew. Chem. Int. Ed.* **2021**, *60*, 13548-13553.

11. Zhou, B.; Xiao, G.; Yan, D., Boosting Wide-Range Tunable Long-Afterglow in 1d Metal-Organic Halide Micro/Nanocrystals for Space/Time-Resolved Information Photonics. *Adv. Mater.* **2021**, *33*,

e2007571.
12. Wu, S.; Zhou, B.; Yan, D., Low-Dimensional Organic Metal Halide Hybrids with Excitation-Dependent Optical Waveguides from Visible to near-Infrared Emission. *ACS Appl. Mater. Interfaces* **2021**, *13*, 26451-26460.
13. Zhao, J.; Zhang, T.; Dong, X. Y.; Sun, M. E.; Zhang, C.; Li, X.; Zhao, Y. S.; Zang, S. Q., Circularly Polarized Luminescence from Achiral Single Crystals of Hybrid Manganese Halides. *J. Am. Chem. Soc.* **2019**, *141*, 15755-15760.
14. Yang, X.; Ma, L. F.; Yan, D., Facile Synthesis of 1d Organic-Inorganic Perovskite Micro-Belts with High Water Stability for Sensing and Photonic Applications. *Chem. Sci.* **2019**, *10*, 4567-4572.
15. Yang, X.; Lin, X.; Zhao, Y.; Zhao, Y. S.; Yan, D., Lanthanide Metal-Organic Framework Microrods: Colored Optical Waveguides and Chiral Polarized Emission. *Angew. Chem. Int. Ed.* **2017**, *56*, 7853-7857.